

STM observation of charge stripe in metallic phase of α -(BEDT-TTF) $_2$ I $_3$ K. Katono,¹ T. Taniguchi,¹ K. Ichimura,^{1,2} Y. Kawashima,¹ S. Tanda,^{1,2} and K. Yamamoto³¹*Department of Applied Physics, Hokkaido University, Sapporo 060-8628, Japan*²*Center of Education and Research for Topological Science and Technology, Hokkaido University, Sapporo 060-8628, Japan*³*Department of Applied Physics, Okayama University of Science, Okayama 700-0005, Japan*

(Received 29 July 2014; revised manuscript received 24 December 2014; published 4 March 2015)

We performed scanning tunneling microscopy at room temperature on the conducting surface of α -(BEDT-TTF) $_2$ I $_3$, which undergoes charge ordering below $T_{CO} = 135$ K. An α -type BEDT-TTF molecular arrangement was clearly observed. We observed a charge stripe structure with some inhomogeneity at room temperature. The horizontal charge stripe developed in most of the observed area. However, the coherence was restricted by the presence of charge uniform regions. The dimerization was found only between A and A' . The charge disproportionation state developed on the donor arrangement, which differs from that in the charge ordered state below T_{CO} . A certain amount of stripe structure inhomogeneity is expected to be caused by the absence of the dimer of B and C BEDT-TTF molecules. We also found a local diagonal stripe that formed the boundary between two types of horizontal stripes.

DOI: [10.1103/PhysRevB.91.125110](https://doi.org/10.1103/PhysRevB.91.125110)

PACS number(s): 71.30.+h, 61.66.Hq, 64.70.kt, 68.37.Ef

I. INTRODUCTION

Charge-transfer salts based on organic donor molecules such as BEDT-TTF and TMTSF have been regarded as a strongly correlated electron system. Organic conductors exhibit various electronic phases [1]. Some of these, including spin-density wave, spin Peierls, and antiferromagnetic phases, result from a strong on-site Coulomb interaction. In κ -(BEDT-TTF) $_2$ X, the superconductivity competes with the Mott insulating phase. These phases have been well described in terms of the on-site Coulomb interaction.

On the other hand, a long-range Coulomb interaction is also important in organic conductors. In fact, the charge ordered (CO) state has been observed [2–4]. The CO state, which is similar to a Wigner crystal, has been discussed theoretically in the extended Hubbard model with the off-site Coulomb interaction [5]. The charge distribution of a CO state is affected by both the long-range Coulomb interaction and the donor arrangement. In α - and θ -type donor arrangements, three types of charge stripe order are plausible. Figure 1 shows schema of the charge stripe patterns. The circles represent donor molecules and their diameters indicate the amount of charge on the donor site. The charge stripe structures are classified by the direction in which the charge aligns, based on donor stacking or column direction. The horizontal stripe has a charge structure in which the charge aligns in the direction perpendicular to the donor stacking. The horizontal stripe structures have been observed with nuclear magnetic resonance (NMR) [6], x-ray diffraction [7], and infrared spectroscopy [8]. However, the results of the observations were macroscopic although they were site-selective measurements. There have been few position sensitive measurements of the CO states in organic conductors [9].

The intermolecular Coulomb interaction also results in charge disproportionation above T_{CO} , and this has been reported in θ -(BEDT-TTF) $_2$ RbZn(SCN) $_4$ and α -(BEDT-TTF) $_2$ I $_3$ [6,7,10,11]. In θ -(BEDT-TTF) $_2$ RbZn(SCN) $_4$, the diffuse spots of $q = (1/3k\ 1/4)$ corresponding to charge disproportionation were observed above T_{CO} . The charge disproportionation is replaced by a horizontal stripe structure

with which structural change occurs with long coherent length when the cooling rate is less than 0.2 K/min. When cooling rate exceeds 5 K/min, the charge disproportionation still remains below T_{CO} . In α -(BEDT-TTF) $_2$ I $_3$, the reported charge disproportionation among A , B , and C BEDT-TTF molecules is far above T_{CO} [7]. The ratio of the charge disproportionation increases with decreasing temperature on the column with B and C BEDT-TTF molecules.

The structural change is associated with the transition from the charge disproportionation state to the CO state. The resistivity [12], charge distribution [7], and permittivity [11] change greatly at T_{CO} , although the long-range Coulomb interaction is independent of temperature. Carriers are localized, and the system becomes an insulator with ferroelectricity below T_{CO} . Therefore, we must clarify the CO state and the charge disproportionation to understand the role of the intermolecular Coulomb interaction and the structural change at the CO transition. The charge disproportionation state without any structural change is very suitable for studying the role of the intermolecular Coulomb interaction. However, the charge distribution of the charge disproportionation, which reflects the effect of the lattice and intermolecular Coulomb interaction, has yet to be clarified in contrast to the CO state. We performed the STM observation on the charge disproportionation in real space on an atomic scale.

Scanning tunneling microscopy (STM) is a powerful tool with which to study the local electronic state, since it probes the local electronic density of states on a nanometer scale without damaging the sample. In fact, it has been used to study the charge modulation of charge density waves (CDWs) in low-dimensional conductors [13] and the checkerboard pattern in cuprate superconductors [14]. In organic conductors, the CDW of TTF-TCNQ has been clearly observed with STM [15]. As the tunneling current gives the local electron density, STM is suitable for studying the CO state in organic conductors. In this study, we focus on α -(BEDT-TTF) $_2$ I $_3$ since the height variation of BEDT-TTF molecules is negligibly small on the α type BEDT-TTF layer in contrast to θ -(BEDT-TTF) $_2$ RbZn(SCN) $_4$.

α -(BEDT-TTF) $_2$ I $_3$ undergoes a CO transition at $T_{CO} = 135$ K [16]. Figure 2(a) shows the layered crystal structure

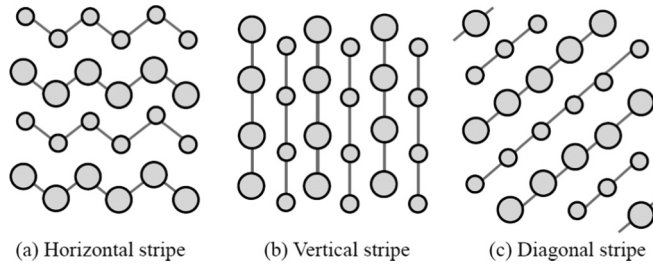


FIG. 1. Schema of the three types of charge order: (a) horizontal stripe, (b) vertical stripe, and (c) diagonal stripe. The circles represent the BEDT-TTF molecules and their diameters express the charge amount on the BEDT-TTF molecules.

of α -(BEDT-TTF) $_2$ I $_3$. Metallic BEDT-TTF and insulating I $_3^-$ layers are stacked alternately along the c axis. Figure 2(b) shows the BEDT-TTF donor layer in the a - b plane. The rectangle in Fig. 2(b) represents the unit cell of the α -type BEDT-TTF molecule arrangement. There are two types of donor stacking columns, which are denoted by I and II, along the a axis. The unit cell contains four BEDT-TTF molecules: $A, A', B,$ and C . Column I consists of A and A' , and column II consists of B and C [12]. It should be noted that A and A' are crystallographically equivalent, and B and C are independent. The structure of CO has been explained as a horizontal stripe with ^{13}C -NMR [6,17], x-ray diffraction [7], and Raman spectroscopy [8]. The first-principle calculation was performed to study the driving force of the CO state [18]. However, the structure of the charge disproportionation has not yet been clarified. X-ray diffraction [7] and Raman spectroscopy [8] suggested that the charge distribution in column I is uniform. On the other hand, ^{13}C -NMR suggested that there is also charge disproportionation on column I [17].

In this paper, we report the charge disproportionation in α -(BEDT-TTF) $_2$ I $_3$ at room temperature that we observed using STM.

II. EXPERIMENTAL

Single crystals of α -(BEDT-TTF) $_2$ I $_3$ were grown with an electrochemical method. Typical dimensions of the single crystals were $1 \times 1 \times 0.5 \text{ mm}^3$. The a - b surface was studied

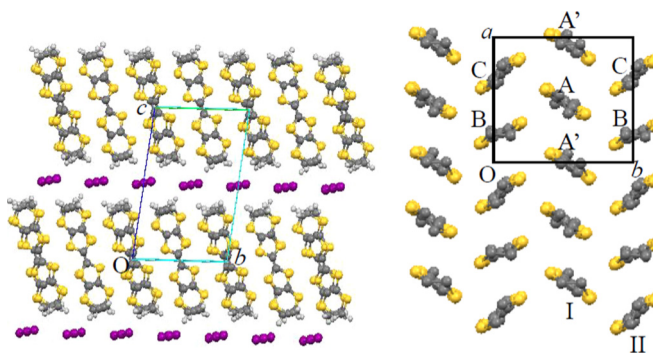


FIG. 2. (Color online) (a) Crystal structure of α -(BEDT-TTF) $_2$ I $_3$ viewed from the b axis. (b) BEDT-TTF arrangement of this salt. Column I consists of BEDT-TTF labeled A and A' . These are crystallographically equivalent. Column II consists of BEDT-TTF labeled B and C .

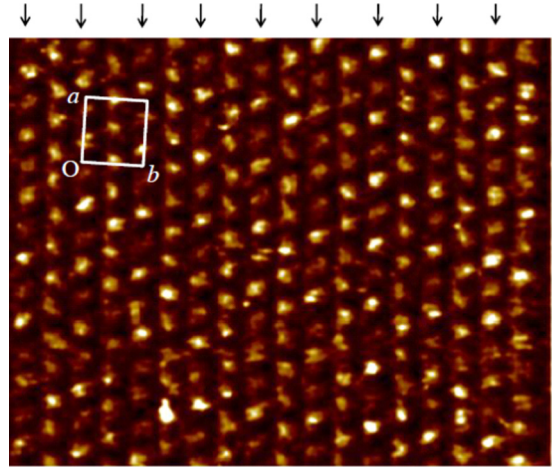


FIG. 3. (Color online) Current image of an a - b plane at bias voltage $V = 50 \text{ mV}$ and tunneling current $I = 50 \text{ pA}$. A white rectangle indicates the unit cell of the BEDT-TTF molecule arrangement in the image.

using STM at room temperature. Tunneling current images were mainly obtained at shiny surfaces. The STM tips were made by cutting Pt-Ir wire, and the resolution was confirmed by observing atomic images of graphite.

III. RESULTS AND DISCUSSION

Figure 3 shows an STM current image of an a - b plane with bias voltage $V = 50 \text{ mV}$ and tunneling current $I = 50 \text{ pA}$. The scanning area is $9.4 \times 6.2 \text{ nm}^2$. The face-centered rectangular pattern was clearly observed. The pattern corresponds to an α -type donor arrangement. The periodicity of the spots is consistent with the lattice parameters, $a = 9.187 \text{ \AA}$, $b = 10.793 \text{ \AA}$, of α -(BEDT-TTF) $_2$ I $_3$. The a and b directions are assigned as indicated in Fig. 3. From the shape of the spots, the slant alternation was along the b axis. Then we can distinguish columns I and II.

We observed that the intensity varied depending on the donor site. The tunneling current depends on both the electronic density of states and the distance from the sample to the tip. In α -(BEDT-TTF) $_2$ I $_3$, BEDT-TTF donors are located at the same height on the a - b surface unlike the case of θ -(BEDT-TTF) $_2$ RbZn(SCN) $_4$ [9]. Therefore, the difference in the tunneling current originates from that in the electronic density of states. X-ray-diffraction [7] and ^{13}C -NMR [6,17] measurements showed that the charge on the B molecule is richer than that on the C molecule above T_{CO} . Taking these results into account, we identified brighter (darker) spots as B (C) along the columns indicated by arrows, and the column indicated by arrows is column II and the other is column I. The spots on the diagonally higher (lower) side of the B molecule are temporarily assigned as A' (A) for the discussion.

To discuss the charge disproportionation in detail, we took line profiles along columns I and II. The profiles were averaged over the width of a column (4.6 \AA) to evaluate the charge distribution in each column. Figure 4 shows line profiles. Red and blue lines represent columns I and II, respectively. The twofold periodicity was clearly observed in the line

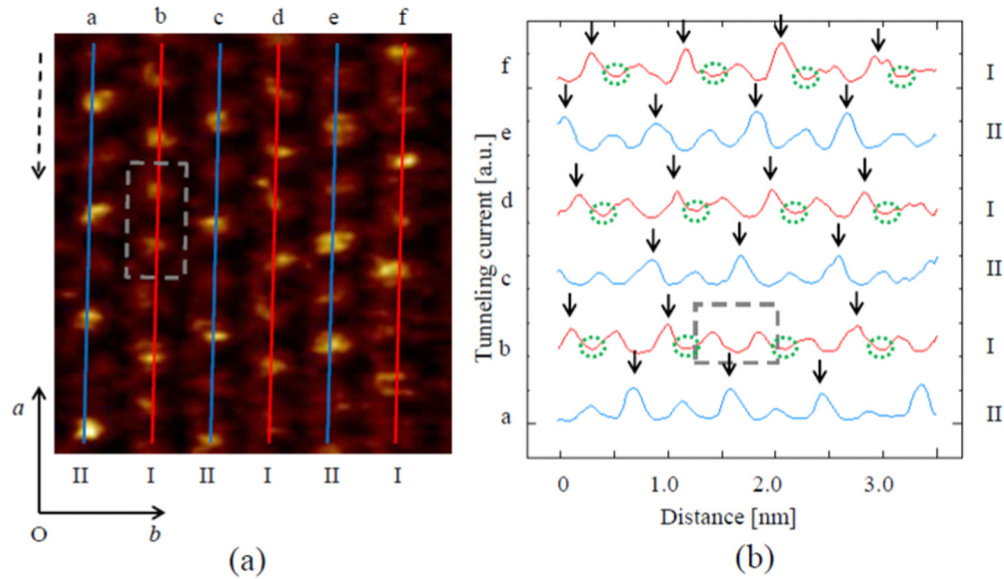


FIG. 4. (Color online) (a) STM image with the same bias voltage and tunneling current. (b) Line profiles along the columns. The arrow on the left in (a) represents the direction of the horizontal axis of (b). Arrows in (b) indicate charge rich molecules. Gray rectangles in (a) and (b) indicate the charge uniform part.

profiles of column II: a, c, and e. Twofold periodicity with charge rich A molecules was also observed in the profiles of column I. The charge disproportionation along columns I and II is consistent with previous work [19]. The twofold periodicities in both columns I and II form a horizontal type stripe structure, which is similar to the structure in the CO state, at room temperature. Moreover, in this study, we found that the stripe structure includes some inhomogeneity by observing the charge distribution on the BEDT-TTF layer in detail. The amplitude of the modulation in column I is weaker than that in column II. The charge amount ratio of the charge rich and poor molecules depends on the position in contrast to the twofold periodicity of column II. A uniform charge distribution domain was observed in the region indicated by the rectangle.

It is possible that the observed stripe structure originates from surface reconstruction. Although there might be the surface effect such as antisymmetry of the anion potential on BEDT-TTF, the surface reconstruction can be excluded. In organic conductors, both intermolecular and intramolecular surface reconstruction are expected to occur, since the donor and anion molecules also consist of many atoms. Ethylene groups of a BEDT-TTF molecule in bulk are distorted due to the anion layer. On the other hand, the ethylene groups closest to the surface are not distorted, since they are not affected by anion molecules. Such surface reconstructions have been reported by an STM study of an organic conductor β -(BEDT-TTF)₂PF₆ [20]. The intermolecular case was observed as an arrangement of alternating bright and less bright columns. The surface reconstruction can be explained as resulting from a mechanism similar to that of Si(100) and GaAs(100). For the higher columns, a large spot was observed that corresponds to a BEDT-TTF molecule with a relaxed ethylene group closest to the surface. For the lower columns two spots with different sizes and brightness levels were observed as a nonrelaxed BEDT-TTF molecule. One is a large bright spot, and the other is a small and less bright spot. In our STM results, only relaxed

BEDT-TTF molecules were observed. If the horizontal stripe is the pattern of the height variation due to intermolecular surface reconstruction, the spots of the nonrelaxed BEDT-TTF molecules must be also observed at the less bright peak of twofold modulation. Therefore, the horizontal stripe was expected to originate from charge.

Next, we note the dips along column I. The shallow dips along column I are indicated by green circles in Fig. 4(b). The shallow and deep dips are aligned alternately along column I. This indicates the dimerization between A and A'. On the other hand, such an alternation of dips was not observed along column II. We emphasize that the dimerization observed with STM reflects the electronic state. The electron density between BEDT-TTF molecules corresponds to the transfer integral. In an α -type donor arrangement above T_{CO} , while molecules A and A' are weakly dimerized, molecules B and C are not. At T_{CO} , x-ray-diffraction measurements suggested a rearrangement of donor molecules that results in dimerization even between B and C, whose transfer integral is almost equal to that of the A-A' dimer [3,7]. Our STM observation of the donor arrangement is consistent with crystallographical results [12] above T_{CO} and indicates that there is no donor rearrangement in contrast to that below T_{CO} . We conclude that the charge disproportionation state develops on the donor arrangement, which is unlike that at the CO state below T_{CO} . We notice that the horizontal stripe observed at room temperature exhibited some inhomogeneity. From the permittivity measurement in θ -(BEDT-TTF)₂RbZn(SCN)₄ [11], T_{CO} decreases as the cooling rate increases, which suppresses the coherence of the structural change such as the dimerization between B and C. Moreover, x-ray-diffraction measurements suggested that the diffuse spots of $q = (1/3 k 1/4)$ corresponding to charge disproportionation still remain below T_{CO} for a fast cooling rate (9–10 K/min) in contrast to the case with a slow cooling rate (0.1–0.2 K/min). These results suggested that the dimerization plays an important role in stabilizing the charge stripe with the

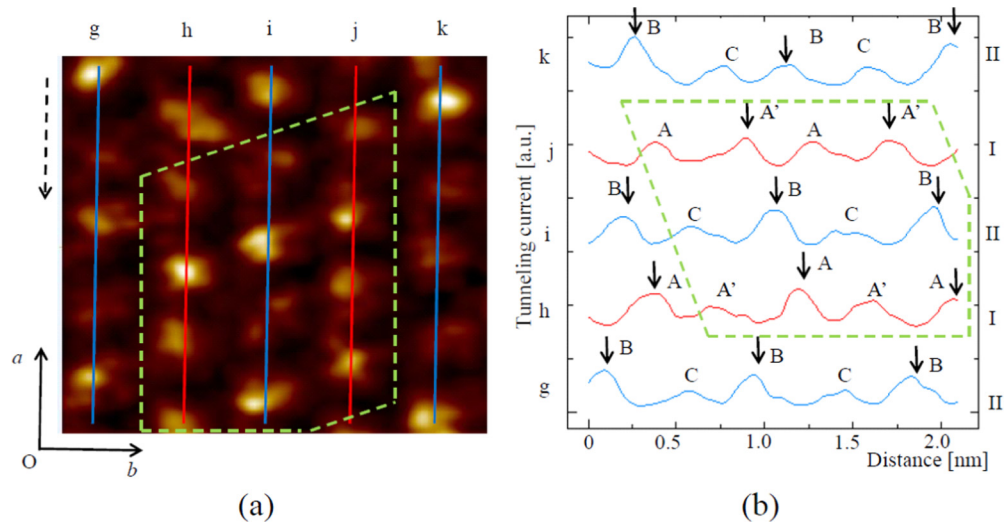


FIG. 5. (Color online) (a) STM image around column I developing twofold periodicity with charge rich A' molecules. (b) Line profiles in (a). The arrow with the broken line represents the direction of the horizontal axis of (b). The arrows in (b) indicate charge rich molecules.

long-range order below T_{CO} and therefore a certain amount of the charge stripe inhomogeneity expected to originate from the absence of the dimerization between B and C .

X-ray-diffraction measurements suggest that the charge distribution on column I is uniform at room temperature [7]. NMR measurements [17] revealed only a slight difference between the charge amounts of the A and A' sites. Our STM method could probe a locally ordered charge stripe with inhomogeneity. The stripe structure in the figure, in which molecules A' are charge rich, was also observed in a different area. Figure 5 shows the line profiles in the area in which we observed the stripe structure with charge rich A' molecules. The twofold periodicity develops over the entire area in Fig. 5(a).

We noticed that the phase of the charge modulation in profile “j” is an inversion of that in profile “h.” The charge modulation in profile “h” is twofold periodicity with charge rich A molecules, which is the same as that in Fig. 4, while the A' site is rich in profile “j.” The twofold periodicity with the charge rich A' molecules forms the stripe structure. A horizontal stripe structure with charge rich A' molecules was formed in columns i, j, and k. In the area surrounded by the

green line in Fig. 5(a), which corresponds to the boundary between A rich and A' rich horizontal stripes, A (column h), B (column i), and A' (column j) molecules are charge rich sites. They form a diagonal stripe [Fig. 1(c)].

We mapped the charge distribution to evaluate the stripe pattern. We reexamined the current image (Fig. 3) in Figs. 6(a) and 6(b). Figure 6(a) shows an STM current image. We mapped the donor sites in Fig. 6(b) and classified them into three types, namely, charge rich, poor, and unclassified sites. Red, blue, and white ellipses represent charge rich, poor, and unclassified sites, respectively. In some parts of column I, the charge is regarded as being uniform as indicated by the white rectangle with broken lines in Fig. 6(a) and the white ellipses in Fig. 6(b). This corresponds to an unclassified site. The twofold periodicity along column II with charge rich B molecules develops over the entire observed area. We note again that the alternation in column II is strict, i.e., site B is charge rich and C is poor. The horizontal stripe structure with charge rich A molecules develops in most of the observed area. In column I, the modulation of the twofold periodicity is weaker than that in column II as described above. The ratio of the electron density on the charge rich and poor molecules varies depending on

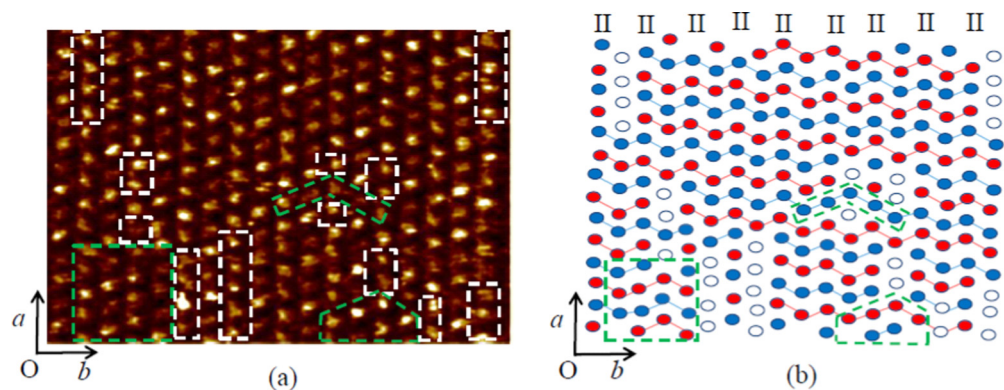


FIG. 6. (Color online) (a) Schema of domain structure. The domain boundaries between stripe structures are projected onto the STM current image of Fig. 3. (b) Schema of donor sites. Red, blue, and white ellipses represent the charge rich, poor, and unclassified sites, respectively.

position in contrast to that in column II as shown in Figs. 4 and 5. In the parts of column I denoted by white ellipses in Fig. 6(b), the alternation between charge rich and poor is not clear. Then it appears that although an A site rich horizontal stripe order develops over almost the whole observed area the coherence is divided by nonclassified sites, in which no charge disproportionation occurs. Additionally, in the green rectangle in Figs. 6(a) and 6(b), diagonal stripes are formed locally. Both A rich and A' rich horizontal stripes are degenerated since A and A' molecules are crystallographically equivalent. It is possible that an A' rich horizontal stripe develops in other areas. Diagonal stripes are formed on the boundary between A rich and A' rich horizontal stripes. The domains with different charge rich molecules have been observed below T_{CO} as the domains with different polarization with optical second-harmonic generation measurement [21]. Even in the CO state, it is expected that a diagonal stripe exists as a domain wall between the domains of the horizontal stripe structures with charge rich A and A' .

We note that the donor arrangement is different from that below T_{CO} . As we mentioned above, B and C molecules along column II form dimers in a CO state. In θ -(BEDT-TTF)₂RbZn(SCN)₄, which is a typical CO compound, charge disproportionation was observed by x-ray diffraction [10]. It is also reported that the T_{CO} of θ -(BEDT-TTF)₂RbZn(SCN)₄ is closely related to the coherence length of the superstructure along the c axis [11]. From these results, we can expect that there is charge disproportionation with some inhomogeneity above T_{CO} , and the charge pattern becomes stable as a result of donor rearrangement. Therefore, our data suggest

that the stripe structure observed with STM is caused by an electron-electron Coulomb interaction between nearest-neighbor molecules, and some inhomogeneity of the stripe structure is caused by the absence of the dimers of B and C molecules along column II.

To investigate this stripe structure and evaluate the charge disproportionation in detail, we must determine the local density of states by performing scanning tunneling spectroscopy on each BEDT-TTF molecule.

IV. CONCLUSION

STM measurement was performed on the a - b plane of α -(BEDT-TTF)₂I₃ at room temperature. The α -type BEDT-TTF donor arrangement was clearly observed. We found a stripe structure with some inhomogeneity in the charge disproportionation phase. The horizontal charge stripe develops in most of the observed area. Dimerization was found between the A and A' molecules. The charge disproportionation state develops on the donor arrangement, which differs from that at the CO state below T_{CO} . The absence of the dimerization between B and C causes some inhomogeneity of the stripe structure. We also found a local diagonal stripe that formed the boundary between two types of horizontal stripe.

ACKNOWLEDGMENTS

This work was partially supported by Grants-in-Aid for Challenging Exploratory Research (Grant No. 24654095) from the Japan Society for the Promotion of Science.

-
- [1] T. Ishiguro, K. Yamaji, and G. Saito, *Organic Superconductors* (Springer, Berlin, 1998).
 - [2] K. Hiraki and K. Kanoda, *Phys. Rev. Lett.* **80**, 4737 (1998).
 - [3] Y. Nogami, R. Moret, J.-P. Pouget, Y. Yamamoto, K. Oshima, K. Hiraki, and K. Kanoda, *Synth. Met.* **102**, 1778 (1999).
 - [4] K. Yamamoto, K. Yakushi, K. Miyagawa, K. Kanoda, and A. Kawamoto, *Phys. Rev. B* **65**, 085110 (2002).
 - [5] H. Seo, *J. Phys. Soc. Jpn.* **69**, 805 (2000).
 - [6] T. Kawai and A. Kawamoto, *J. Phys. Soc. Jpn.* **78**, 074711 (2009).
 - [7] T. Kakiuchi, Y. Wakabayashi, H. Sawa, T. Takahashi, and T. Nakamura, *J. Phys. Soc. Jpn.* **76**, 113702 (2007).
 - [8] Y. Yue, K. Yamamoto, M. Uruichi, C. Nakano, K. Yakushi, S. Yamada, T. Hiejima, and A. Kawamoto, *Phys. Rev. B* **82**, 075134 (2010).
 - [9] K. Ichimura, S. Ikeda, M. Kawai, K. Nomura, J. Ishioka, and S. Tanda, *Physica B* **404**, 570 (2009).
 - [10] M. Watanabe, Y. Noda, Y. Nogami, and H. Mori, *Synth. Met.* **135**, 665 (2003).
 - [11] F. Nad, P. Monceau, and H. M. Yamamoto, *Physica B* **404**, 473 (2009).
 - [12] K. Bender, I. Hennig, D. Schweitzer, K. Dietz, H. Endres, and H. J. Keller, *Mol. Cryst. Liq. Cryst.* **108**, 359 (1984).
 - [13] R. V. Coleman, *Adv. Phys.* **37**, 559 (1988).
 - [14] T. Hanaguri, C. Lupien, Y. Kohsaka, D. H. Lee, M. Azuma, M. Takano, H. Takagi, and J. C. Davis, *Nature (London)* **430**, 1001 (2003).
 - [15] Z. Z. Wang, J. C. Girard, C. Pasquier, D. Jerome, and K. Bechgaard, *Phys. Rev. B* **67**, 121401(R) (2003).
 - [16] K. Kajita, Y. Ojiro, H. Fujii, Y. Nishino, H. Kobayashi, A. Kobayashi, and R. Kato, *J. Phys. Soc. Jpn.* **61**, 23 (1992).
 - [17] S. Moroto, K.-I. Hiraki, Y. Takano, Y. Kubo, T. Takahashi, H. M. Yamamoto, and T. Nakamura, *J. Phys. IV France* **114**, 399 (2004).
 - [18] P. Alemany, J. P. Pouget, and E. Canadell, *Phys. Rev. B* **85**, 195118 (2012).
 - [19] E. Mori, H. Usui, H. Sakamoto, K. Mizoguchi, and T. Naito, *J. Phys. Soc. Jpn.* **81**, 014707 (2012).
 - [20] M. Ishida, O. Takeuchi, T. Mori, and H. Shigekawa, *Phys. Rev. B* **64**, 153405 (2001).
 - [21] K. Yamamoto, A. A. Kowalska, and K. Yakushi, *Appl. Phys. Lett.* **96**, 122901 (2010).